Electrospun Poly(L-lactide)/Poly(ε-caprolactone) Blend Fibers and Their Cellular Response to Adipose-Derived Stem Cells

Gui-Ying Liao,[1] Liang Chen,[2] Xiao-Yong Zeng,[2] Xing-Ping Zhou,[1] Xiao-Lin Xie,[1] E-Jun Peng,[2] Zhang-Qun Ye,[2] Yiu-Wing Mai[3]

[1]*Hubei Key Laboratory of Materials Chemistry and Service Failure, School of Chemistry and Chemical Engineering, Huazhong University of Science and Technology, Wuhan, People's Republic of China*
[2]*Department of Urology, Tongji Hospital, Tongji Medical College, Huazhong University of Science and Technology, Wuhan, People's Republic of China*
[3]*Center for Advanced Materials Technology (CAMT), School of Aerospace, Mechanical and Mechatronic Engineering J07, University of Sydney, Sydney, New South Wales, Australia*

Received 21 May 2010; accepted 12 September 2010
DOI 10.1002/app.33398
Published online 9 December 2010 in Wiley Online Library (wileyonlinelibrary.com).

ABSTRACT: Polymer blending is one of the most effective methods for providing new, desirable biocomposites for tissue-engineering applications. In this study, electrospun poly(L-lactide)/poly(ε-caprolactone) (PLLA/PCL) blend fibrous membranes with defect-free morphology and uniform diameter were optimally prepared by a 1 : 1 ratio of PLLA/PCL blend under a solution concentration of 10 wt %, an applied voltage of 20 kV, and a tip-to-collector distance of 15 cm. The fibrous membranes also showed a porous structure and high ductility. Because of the rapid solidification of polymer solution during electrospinning, the crystallinity of electrospun PLLA/PCL blend fibers was much lower than that of the PLLA/PCL blend cast film. To obtain an initial understanding of biocompatibility, adipose-derived stem cells (ADSCs) were used as seed cells to assess the cellular response, including morphology, proliferation, viability, attachment, and multilineage differentiation on the PLLA/PCL blend fibrous scaffold. Because of the good biocompatibility and nontoxic effect on ADSCs, the PLLA/PCL blend electrospun fibrous membrane provided a high-performance scaffold for feasible application in tissue engineering using ADSCs.
 J Appl Polym Sci 120: 2154–2165, 2011

Key words: poly(L-lactide)/poly(ε-caprolactone); blend; electrospinning; scaffold; adipose-derived stem cells

INTRODUCTION

Tissue engineering is a multidisciplinary area that has evolved in parallel with recent advances in materials and biotechnology. Particularly, electrospun nano- and microscale nonwoven polymer fibrous mats are widely used as scaffolds for tissue engineering.[1,2] Electrospinning is a simple, relatively efficient, technique to fabricate polymer fibers with less than 50 nm to over 1 μm diameter, which are mostly spun from polymer solutions.[3–6] Because the morphologies and surface properties of electrospun fibers depend on the physical parameters of the polymer solution (e.g., concentration, viscosity, conductivity, and surface tension) and the spinning process parameters (e.g., applied voltage, distance between capillary tip and collection screen, temperature, and humidity of the ambient environment),[7–9] optimization of the above parameters is a major challenge in preparing high-performance nonwoven polymer fibrous mats as scaffolds for tissue engineering applications. Also, and most importantly, the materials must be biodegradable and biocompatible.[2] Recently, polymeric biomaterials, such as poly (lactic acid) (PLA), poly(glycolic acid), poly(ε-caprolactone) (PCL), and their copolymers, have attracted great attention because of their distinctive degradation and excellent biocompatibility.[10–13] Of these, PLA is most promising and widely used as candidate scaffolds for tissue engineering.[14] However, its brittleness has limited its wider biomedical applications. PCL is a biodegradable, semicrystalline, and rubbery polymer owing to its low glass transition ($\sim -50°C$) and melting temperatures ($\sim 60°C$).[15] It has been often used to improve the elasticity of PLA via blending[16–18] or block copolymerization.[19–22]

Correspondence to: X.-L. Xie (xlxie@mail.hust.edu.cn) or X.-Y. Zeng (xyzeng@tjh.tjmu.edu.cn).
Contract grant sponsor: National Science Foundation of China; contract grant numbers: 30700171, 50825301.
Contract grant sponsor: Scientific Research Foundation for Returned Overseas Chinese Scholars.
Contract grant sponsor: Scientific Research Foundation of Huazhong University of Science and Technology (HUST).

Until now, most P(LA-*b*-CL) block copolymers are electrospun to nonwoven fibrous mats as scaffolds for the culture of somatic cells, such as smooth muscle cells and endothelial cells (ECs).[19–21] Results obtained showed that these cells could adhere and proliferate well on P(LA-*b*-CL) fibrous scaffolds. Kwon et al.[22] produced nano- and microstructured biodegradable poly(L-lactide-*co*-ε-caprolactone) fabrics by electrospinning and the high-molecular-weight poly(L-lactide-*co*-ε-caprolactone)s by ring-opening copolymerization, and human umbilical vein ECs were well adhered and proliferated on these fabrics. Vaz et al.[23] electrospun a bilayer tubular scaffold composed of oriented stiff PLA fibers as the outer shell and random flexible PCL fibers as the inner core to mimic the structure of a blood vessel, and found that the PLA/PCL bi-layer scaffold as a prototype for blood vessel tissue engineering was capable of supporting the attachment, spreading, and growth of mouse fibroblasts and human myofibroblasts. However, there are very few studies on electrospinning of PLA/PCL blends, and indeed only PLA/PCL blend cast films were previously prepared as engineered tissue implants.[16,24,25] Compared with block copolymerization, polymer blending is one of the simpler and more effective methods for providing new, desirable biomaterials for tissue-engineering applications. Thus, in this study, we focus on optimization of the preparation of poly(L-lactide) (PLLA)/PCL blend scaffold and examination of their cellular biocompatibility. There are some published works on the biocompatibility of biodegradable scaffolds, such as P(LA-*b*-CL) nanofibers, PLA/PCL blend films, PCL foams, PLA particles, etc. with somatic cells, such as smooth muscle cell,[19,26] EC,[19,20] fibroblasts, osteoblast cells,[24] hepatocytes,[25] urinary tract stromal cells,[27] Jurkat and HeLa cells,[28] etc. However, the response of stem cells on PLLA/PCL blend fibers has not been studied.

At the core of tissue engineering, stem cells play a critical role in regenerative medicine owing to their ability to self-renew and differentiate along multiple lineage pathways.[14,29,30] Compared with embryonic and bone marrow stem cells, adipose-derived stem cells (ADSCs) can be isolated from the adipose tissue, which overcomes the ethical and political issues that accompany the use of embryonic stem cells.[31] Because of their abundant quantity, less immunity, minimal invasive procedure, low morbidity, easy isolation, and rapid proliferation, ADSCs have paved a new efficient path for regenerative medicine since they were isolated and characterized by Zuk et al.[32] As an important and convenient source of stem cells, ADSCs are usually used as seed cells for investigation of scaffold performance in tissue engineering.

In this work, we electrospun PLLA/PCL blend fibers and studied the effects of the weight ratio of PLLA to PCL, concentration of solution, applied voltage, and tip-to-collector distance (TCD) on the morphology and diameter of the electrospun fibers. To obtain a fundamental understanding of the biocompatibility of the optimal spun fibers, we selected ADSCs as seed cells to assess the cell morphology and proliferation, viability, attachment, and differentiation capability on the PLLA/PCL blend fibrous scaffold.

MATERIALS AND METHODS

Materials

PLLA with an average molecular weight M_w of 100,000 was supplied by Shenzhen Guanghua Co. Ltd., China. PCL with an average molecular weight M_w of 1000 was purchased from Slovey Co., South Korea. Phosphate buffered saline (PBS), collagenase type I, and Dulbecco's modified Eagle's medium (DMEM) were obtained from Gibco Co. (Grand Island, NY). MCDB 131 medium and heparin were purchased from Sigma Co. (St. Louis, MO). Fetal bovine serum was purchased from Hyclone Co. (Logan, UT). Trypsin/ethylene diamine tetra-acetic acid (EDTA), 3-(4,5-dimethylthiazol-2-yl)-2,5-diphenyltetrazolium bromide (MTT), Hoechst 33342, and propidium iodide were supplied by Invitrogen Co. (Carlsbad, CA). The immunohistochemistry reagents and all the components of differentiation medium except DMEM were purchased from Sigma-Aldrich Co. (St. Louis, MO). Solvents, chloroform, dimethyl sulfoxide, and methanol were all analytical-grade reagents. All materials were used without further purification.

Preparation of PLLA/PCL blend fibers

PLLA/PCL blend solutions with a range of different blending composition (Samples 1–4 in Table I) and concentration (Samples 3 and 5–7 in Table I) were prepared by dissolving PLLA and PCL in a solvent of chloroform and methanol (~ 3/1 volume ratio), followed by magnetic stirring for 4 h at ambient temperature.

The polymer solution was added to a 2-mL syringe with a needle having an inner diameter of 0.46 mm. The electrical field was provided by a DW-P353-3ACCD high-voltage power supply (Tianjin High Voltage Technology Factory, China), which could give voltages from 0 to 30 kV. A copper wire connected to the positive electrode was inserted into the polymer solution, and a grounded aluminum foil as collector was positioned opposite and perpendicular to the needle tip. Mass flow rate of solutions was 1.0 mL/h. All electrospinning experiments were

TABLE I
Solution Properties of PLLA/PCL Blends and the Morphology of Fibers

Sample number	PLLA/PCL ratio	Concentration (wt %)	Conductivity (μS/cm)	Surface tension (mN/m)	Viscosity (Pa·s)	AD (nm)	Fiber morphology
1	3/1	10	0.73	24.07	0.188	~ 4360	Fiber
2	2/1	10	0.67	22.25	0.128	~ 2140	Fiber
3	1/1	10	0.63	21.85	0.051	780 ± 24	Fiber
4	1/2	10	0.61	20.43	0.026	180–750	Beaded fibers
5	1/1	6	0.93	12.91	0.014	234 ± 72	Beaded fibers
6	1/1	8	0.75	14.90	0.030	304 ± 31	Few beads
7	1/1	12	0.48	21.91	0.098	818 ± 30	Fiber

performed at ambient temperature, and the relative humidity was 40–60%.

To compare with electrospun PLLA/PCL blend fibers, PLLA/PCL films were also made by solution casting, then held at ambient temperature for 24 h, and dried in vacuum at 30°C overnight.

Characterization of PLLA/PCL blend solutions, electrospun fibers, and cast films

The surface tension of the PLLA/PCL blend solutions was tested using a K99B tensiometer (Schmidt, Germany) at ambient temperature. The solution electrical conductivity was determined by a Cond730 conductivity instrument (Shanghai, China), and the solution viscosities were measured at 20°C and 80 rpm with a Brookfield R/S Rheometer (Brookfield, Middleboro, MA). The porosity (ε) of the electrospun fibrous membrane was determined by the density method.[33]

The morphology of the electrospun fiber was observed by a Quanta 400 scanning electron microscope (Phillips, the Netherlands). The specimen was coated with a thin gold layer before scanning electron microscopy (SEM) examination. The fiber average diameter (AD) was statistically calculated by analyzing 20 fibers at random, and the average value reported with standard deviations.

X'Pert Pro X-ray diffractometer (Phillips) with Cu Kα radiation ($\lambda = 1.5406$ Å) at a generator voltage of 40 kV and a current of 40 mA was used to analyze the crystallinity properties of the electrospun fibers and the cast films. All experiments were conducted in the 2θ range of 10–30° at ambient temperature, with a scanning speed of 5°C/min and step size of 0.02°.

The thermal behaviors of the electrospun fibers and cast films were studied with a Diamond differential scanning calorimeter (Perkin–Elmer, Waltham, MA) at a heating rate of 10°C/min in dry nitrogen atmosphere.

Tensile properties of the electrospun fibrous membranes of PLLA and PLLA/PCL (1/1) blend and their cast films were obtained on rectangular specimens 80 × 20 mm^2 in a CMT-4104 universal testing machine (Shenzhen, China) at a crosshead speed of 10 mm/min under ambient conditions. The average value of five repeated tests was taken for each material composition.

ADSCS isolation and culture

ADSCs were isolated using a modified method reported by Gimble and Guilak.[34] Five New Zealand white rabbits (two male and three female, aged 3.8–4.2 months, weighed 1.8–2.4 kg) were used in the following test. The Medical Ethics Committee of Tongji Medical College of Huazhong University of Science and Technology (Wuhan, China) approved the use of animals. Briefly, rabbit subcutaneous adipose tissues in the inguinal region were resected, washed with PBS extensively to remove red blood cells, then chopped to small pieces ~ 1–2 mm^3 in size, digested with 1 mg/mL collagenase type I for 2 h at 37°C with continuous shaking, and filtered through a 100-μm (pore size) mesh to remove the debris. The ADSCs-containing fraction was separated from the floating adipocytes using multiple centrifugal and washing steps. The harvested cells were plated at 2 × 10^4 cells/cm^2 in per 25-cm^2 culture flasks (Corning Inc., Corning, NY) filled with 5 mL culture medium composed of DMEM that was supplemented with 10% fetal bovine serum, 100 unit/mL of penicillin, and 100 μg/mL of streptomycin. The culture flasks were placed in an incubator (Thermo Scientific, San Jose, CA) at 37°C and 5% CO_2, and the medium was replaced completely every 3 days. After reaching 80% confluence, the cells were passaged by 0.25% trypsin/EDTA in PBS. ADSCs at their fourth to sixth passages were used in this study. Flow cytometry analyses showed that the cells were $CD34^-$ and $CD45^-$, and $CD105^+$ and $CD166^+$, which indicated the typical profile of stem cell markers.

Cell seeding

Before cell seeding of ADSCs, the electrospun fibrous membranes as cell scaffolds were cut into square pieces of 5 × 5 mm^2 in size. All pieces of

scaffolds were sterilized by soaking in 75% alcohol for 1 h, and washing in PBS for 10 s.

ADSCs were released by 0.25% trypsin/EDTA and measured by a blood cell counter, and the resulting number was the average from three tests. The ADSCs-containing suspension was seeded fibrous scaffolds, which were placed on the bottom of eight 96-well tissue culture plates (Costar, Cambridge, MA). The seeding density was 2×10^4 cells/mL in 200 μL culture medium per well. The cellular constructs were maintained in a humidified incubator with 5% CO_2 at 37°C, and the medium was replaced every 3 days.

Cell morphology

The behavior of ADSCs on scaffold was visualized by a CK40 inverted phase contrast microscope (Olympus, Japan) at random locations in a 96-well tissue culture plate. The cellular constructs were, respectively, harvested after 1, 3, and 7 days seeding, washed with PBS to remove nonadherent cells, fixed by 4% glutaraldehyde for 1 h at ambient temperature, dehydrated via a series of gradient alcohol solutions, and then dried in vacuum. Dry constructs were sputter-coated with gold and observed using SEM.

Cell proliferation

For proliferation investigation, the remaining seven 96-well tissue culture plates were assessed by MTT assay. Each plate was loaded with five replicate wells of ADSCs-scaffold constructs and five replicate wells of nonseeding ADSCs as controls. After cell seeding, one culture plate per day was removed from the incubator in 7 days, added with 10 μL MTT solution, incubated at 37°C for 4 h, and then 100 μL formazan reagent was added to dissolve the formed crystals. The optical density (OD) was measured by absorbance at 490 nm with a MK3 microplate reader (Thermo Scientific).

Cell viability and attachment

Two ADSCs-scaffold constructs in the first 96-well tissue culture plate used in cell morphology were transferred to a new 96-well plate on the first and seventh day after seeding, respectively. The constructs were incubated in PBS containing Hoechst 33342 and propidium iodide for 0.5 h to label the viable (blue fluorescence) and necrotic (red fluorescence) cells, respectively. Nonseeded ADSCs in conventional culture were submitted to identical conditions. Images were observed and recorded by a FV500 confocal laser scanning microscope (Olympus) coupled with a TS-100 digital camera (Nikon, Japan). Three randomly chosen view regions were photographed for each film, and the live ADSCs were counted. The received percentage of live cells (P_{Live}) was used to characterize the cell viability, and the cell attachment number of live cells per scaffold surface of (C_{Attach}) was used to characterize the cell attachment density. The results presented were the average from three tests.

Multilineage differentiation of ADSCs

To evaluate the performance of such electrospun scaffold, the expanded ADSCs on scaffolds were analyzed by immunohistochemistry staining for osteogenic and adipogenic differentiation, which represent typical differentiation capacity of stem cells. After seeding ADSCs on the fibrous scaffolds for 7 days, six constructs in the first 96-well tissue culture plate were transferred to two new Petri dishes (three constructs per dish) to be cultured in an inductive medium. For osteogenic differentiation, the medium consisted of 0.01 μ*M* 1,25-dihydroxyvitamin D, 50 μ*M* ascorbate-2-phosphate, 10 m*M* β-glycerophosphate, and 1% antibiotic/antimycotic in DMEM. For adipogenic differentiation, the medium consisted of 0.5 m*M* isobutyl-methyl-xanthine, 1 μ*M* dexamethasone, 10 μ*M* insulin, 200 μ*M* indomethacin, 1% antibiotic/antimycotic in DMEM. Both inductive media were refreshed every 3 days. Osteogenic differentiation was evaluated at 3 weeks by the histochemical presence of mineralized extracellular matrix (ECM) using von Kossa staining, and adipogenic differentiation was assessed at 2 weeks by detection of fatty substance accumulation using oil red O staining.

RESULTS AND DISCUSSION

Morphology of PLLA/PCL electrospun fibrous scaffolds

PLLA/PCL blend solutions with different blending weight ratio, varying from 3/1 to 1/2 (Samples 1–4 in Table I), were prepared. Figure 1 shows SEM images of electrospun fibers under solution concentration of 10 wt %, voltage 20 kV, and TCD 15 cm. When the PLLA/PCL blending weight ratio is 3/1, a smooth fiber with an AD of $\sim$ 4.36 μm is electrospun [Fig. 1(a)]. With increasing PCL content in the PLLA/PCL blends, the AD decreases significantly. For PLLA/PCL blend with weight ratio 2/1, the AD of electrospun fibers is $\sim$ 2.14 μm [Fig. 1(b)]. For PLLA/PCL blend with weight ratio 1/1, the AD of the electrospun fibers is 780 $\pm$ 24 nm [Fig. 1(c)]. However, when the PLLA content in the PLLA/PCL blends is decreased to 33.3 wt % (i.e., the blending weight ratio is 1/2), beads appear in the electrospun PLLA/PCL blend fibers with widely distributed diameters varying from 180 to 750 nm [Fig. 1(d)].

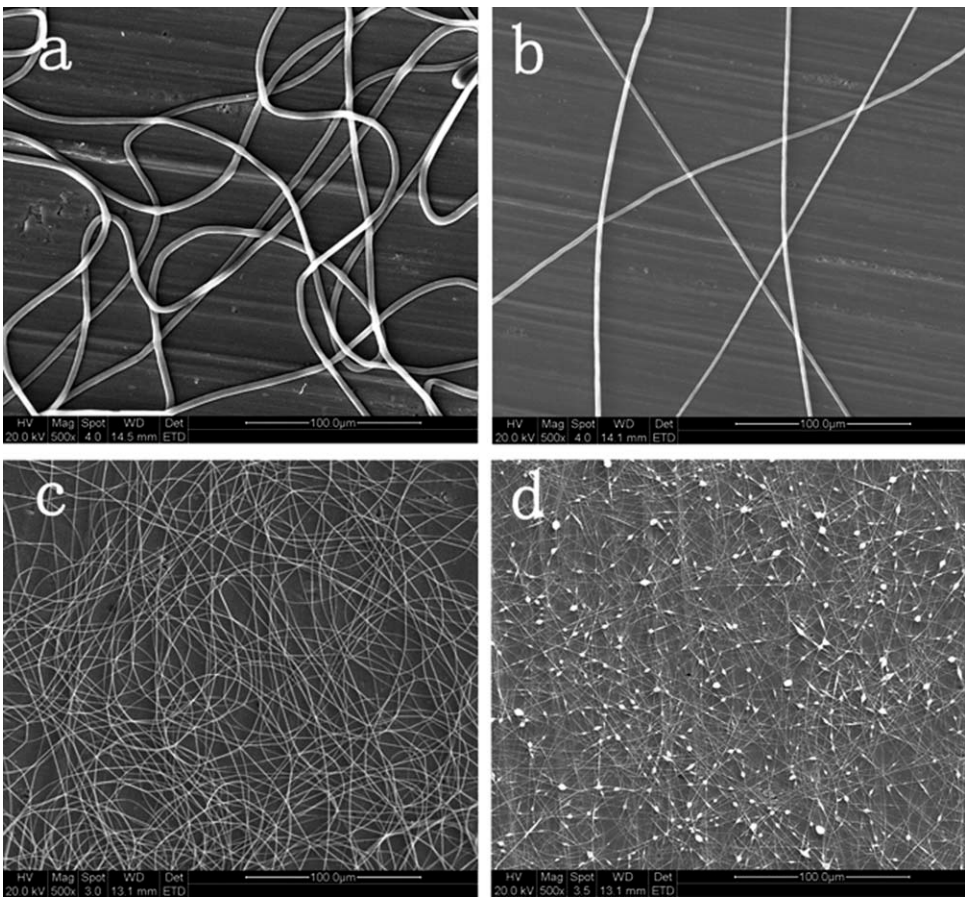

Figure 1 SEM micrographs of electrospun PLLA/PCL blend fibers at solution concentration of 10 wt %, voltage 20 kV, and TCD 15 cm. (a) PLLA/PCL (3/1), (b) PLLA/PCL (2/1), (c) PLLA/PCL (1/1), and (d) PLLA/PCL (1/2).

Obviously, the morphology and diameter of electrospun fibers are critically affected by the PLLA/PCL blend composition. From Table I (Samples 1–4), the conductivity, surface tension, and viscosity of PLLA/PCL blend solution decrease with decreasing content of PLLA. Especially, the decrement of solution viscosity is the largest. For example, the solution viscosity of PLLA/PCL blend with weight ratio 1/2 decreases by 86.2%, i.e., its solution viscosity decreases to 0.026 Pa·s from 0.188 Pa·s of the PLLA/PCL blend with weight ratio 3/1. Thus, the PLLA content in PLLA/PCL blends reveals a significant effect on electrospinning. The solutions of PLLA/PCL blends with 50% or more PLLA have good electrospinability, and PLLA/PCL blend with weight ratio 1/1 yields the finest electrospun fibers because of its appropriate solution viscosity.[1,8,35]

Figure 2 shows the SEM micrographs of PLLA/PCL (1/1) blend fibers electrospun at different solution concentration (Samples 3 and 5–7 in Table I). Defects such as beads exist in the electrospun fibers with an AD of 234 ± 72 nm when the electrospinning solution concentration is 6 wt % [Fig. 2(a)]. With increasing concentration to 8 wt %, the beads in the electrospun fibers with AD values of 304 ± 31 nm [Fig. 2(b)] change to spindle-like structure. When the solution concentration is further increased to 10 wt %, bead-free smooth fibers with AD 780 ± 24 nm are obtained [Fig. 2(c)]. At 12 wt % solution concentration, the diameter of electrospun fibers increases to 818 ± 30 nm [Fig. 2(d)]. These indicate that a critical concentration (~ 10 wt %) exists in the electrospinning process of PLLA/PCL blend solutions. From Table I (Samples 5–7 and 3), it can be seen that as the solution concentration increases, both the surface tension and viscosity increase but the conductivity decreases. At solution concentrations below the critical 10 wt %, there are fewer chain entanglements because of the low surface tension and viscosity. Also, the high conductivity enables the occurrence of marked fiber jet instability,[2] which leads to unstable electrospinning. However, at solution concentrations more than 10 wt %, the improvement in electrospinability is related to the increase in solution viscosity because of the enhanced chain entanglements[35] and reduced conductivity.[2]

By adjusting the electrospinning conditions, such as applied voltage and TCD, the morphology of the electrospun fibers can be effectively controlled. Figure 3 shows SEM micrographs of fibers electrospun

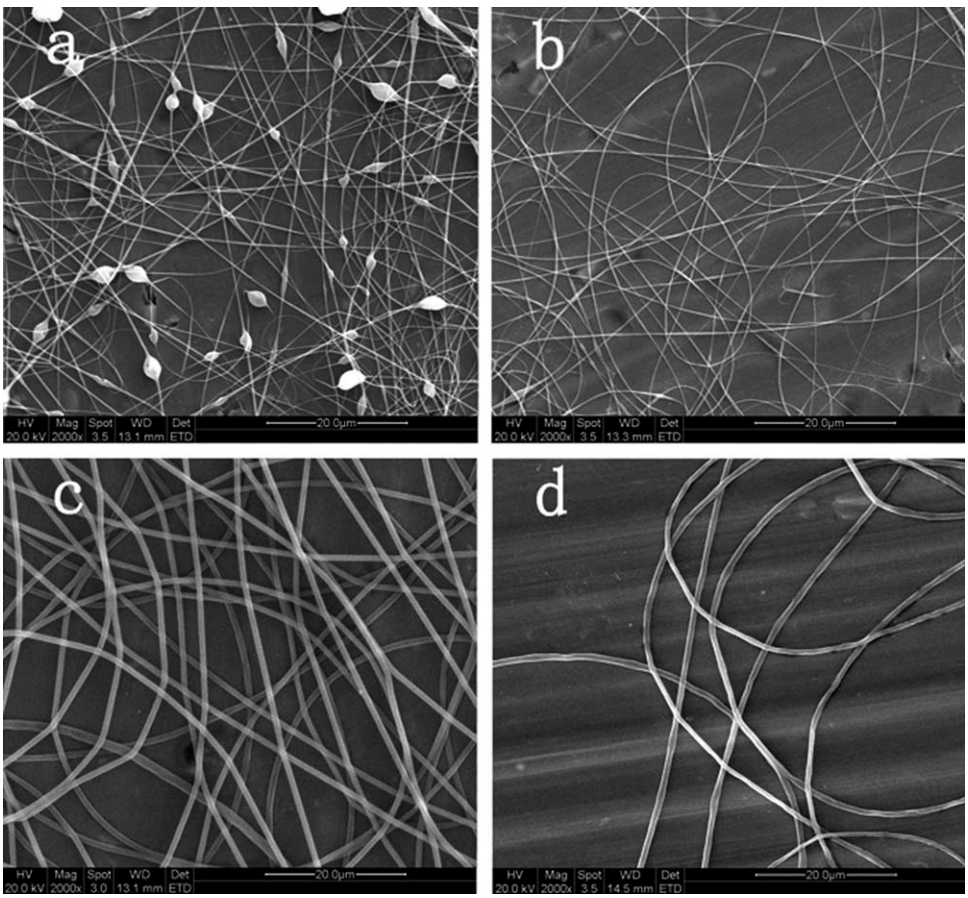

Figure 2 SEM micrographs of fibers electrospun by different solution concentration for PLLA/PCL (1/1) blend at voltage 20 kV and TCD 15 cm. (a) 6 wt %, (b) 8 wt %, (c)10 wt %, and (d) 12 wt %.

at different voltages and TCD for PLLA/PCL (1/1) blend with a solution concentration 10 wt %. As expected, when TCD is set to 15 cm, the electrospun fibers with large diameters and wide distributions are formed (i.e., AD of 987 ± 208 nm) under an applied voltage of 10 kV [Fig. 3(a)]. When the applied voltage is 20 kV, smooth, fine, uniform, and defect-free electrospun fibers with an AD of 780 ± 24 nm are spun [Fig. 3(b)]. Therefore, we can conclude that with increasing applied voltage, the fibers become thinner and more uniform. However, as the voltage is increased to 30 kV [Fig. 3(c)], there exist some beads on the nonuniform fibers with AD of 459 ± 196 nm because of the high drawing stress in the jet. Further, the corona discharge by the high voltage also leads to more neutralizing ions and formation of beads.[8] When the applied voltage is set at 20 kV, there are also obvious differences between the morphologies of the electrospun fibers at TCD from 10 to 20 cm. When TCD is 10 cm, there are some defects, such as aggregations of the fibers, in the nonuniform fibers with an AD of 854 ± 59 nm [Fig. 3(d)] because of inadequate evaporation of the fiber before reaching the collector. When TCD is 15 cm, the finest fibers in Figure 3(b) are obtained. However, when the TCD is further increased to 20 cm, nonuniform fibers are spun with widely distributed diameters varying from 200 to 1000 nm [Fig. 3(e)]. Hence, with increasing TCD, the fiber diameter distribution narrows from 10 to 15 cm but widens again at 20 cm, which is related to the instability and elongation process as the solution jet travels a long distance from the needle tip to the collector.

Crystallinity of eletrospun fibers

Electrospinning is different from other molding processes and provides electrospun fibers with different properties, such as crystallinity. The crystallinity of the above PLLA/PCL (1/1) blend fibers electrospun at solution concentration of 10 wt %, voltage of 20 kV, and TCD of 15 cm was characterized by X-ray diffraction (XRD) and differential scanning calorimetry (DSC). Figure 4 shows the XRD patterns of the electrospun fibers and corresponding cast films of PLLA/PCL (1/1) blend. Obviously, there are two main diffraction peaks at 2θ of 16.9° and 19.2° in the PLLA/PCL blend cast films, which are the characteristic peaks of the α-crystals of PLLA.[13] Furthermore, the blend films have a very weak diffraction peak near 22.3°, which is

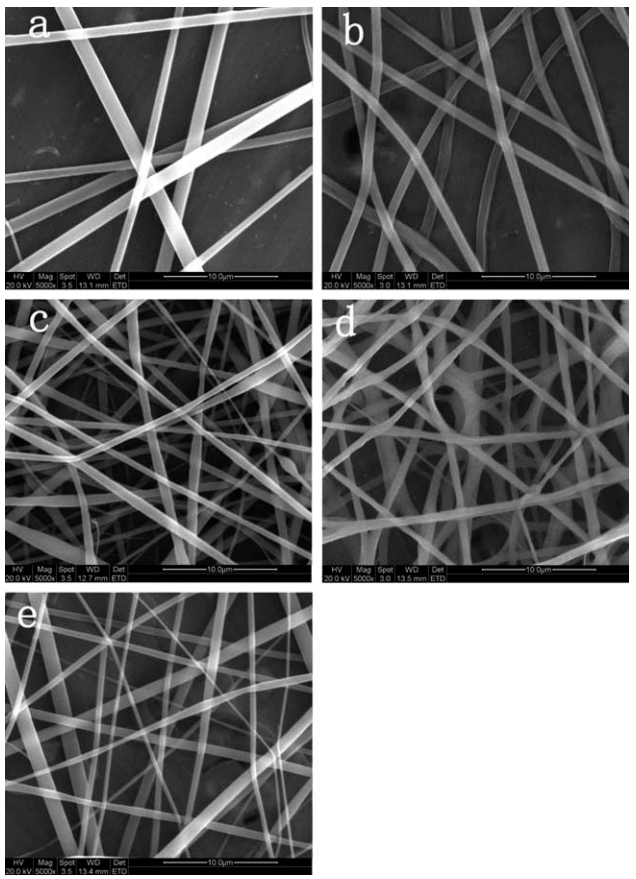

Figure 3 SEM micrographs of fibers electrospun at different voltages and TCDs for PLLA/PCL (1/1) blend at solution concentration 10 wt %. (a) 10 kV, 15 cm; (b) 20 kV, 15 cm; (c) 30 kV, 15cm; (d) 10 cm, 20 kV; and (e) 20 cm, 20 kV.

assigned to the characteristic peak of PCL.[36] However, in the PLLA/PCL blend fibers, the diffraction peaks of PLLA are relatively weak, and the diffraction peak of PCL disappears. The results suggest that the crystalline phase is mainly PLLA phase in these films and fibers, and that the crystallinity of electrospun PLLA/PCL blend fibers is significantly lower than that in the PLLA/PCL blend cast film.

The DSC curves of the above electrospun fiber and cast film of PLLA/PCL (1/1) blend are shown in Figure 5. There exist the weak melting peak of PCL at around 39.0°C with melting enthalpy ΔH_m = 1.46 J/g, cold crystallization peak of PLLA near 82.5°C with crystallization enthalpy $\Delta H_c = -14.4$ J/g, and strong melting peak of PLLA at 139.0°C with melting enthalpy ΔH_m = 23.6 J/g in PLLA/PCL blend cast film. It is noted that the small melting peak at 129.0°C is related to the imperfect α-crystals of PLLA.[37] For electrospun PLLA/PCL blend fibers, there exist only the cold crystallization peak of PLLA near 71.7°C with crystallization enthalpy ΔH_c = −11.2 J/g, and melting peak of PLLA at 137.0°C with melting enthalpy ΔH_m = 19.1 J/g). The degree of crystallinity (χ_c) was calculated based on[17]:

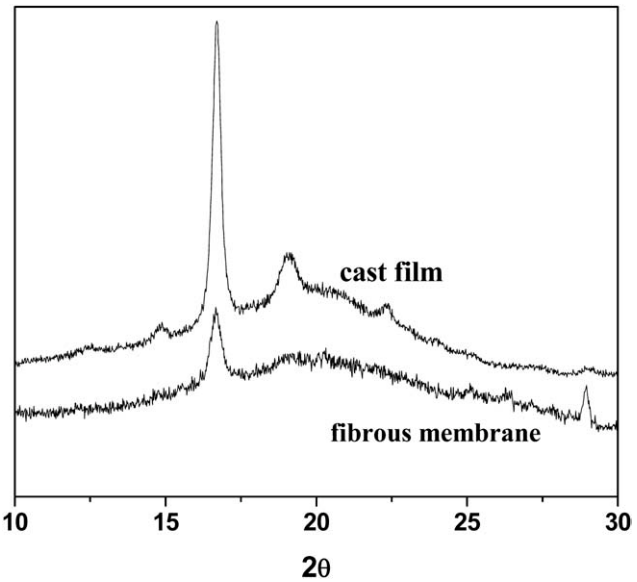

Figure 4 XRD patterns of electrospun fibrous membrane and cast film of PLLA/PCL (1/1) blend.

$$\chi_c = \frac{\Delta H_m - \Delta H_c}{\omega \Delta H^0} \times 100\% \quad (1)$$

where ΔH_m and ΔH_c are the absolute values of melting enthalpy and cold crystallization enthalpy of PLLA crystals, respectively, and ω is the weight fraction of PLLA in the blend. The value of ΔH^0 for 100% crystalline PLLA is 106 J/g.[17,38] Based on DSC experimental data, the χ_c values in the PLLA/PCL blend fibers and cast film are calculated as 14.9% and 17.4%, respectively. Obviously, the crystalline phase is mainly PLLA phase in these films and fibers. The disappearance of the melting peak of PCL, lower melting temperature, and the enthalpy of PLLA in electrospun PLLA/PCL blend fibers all

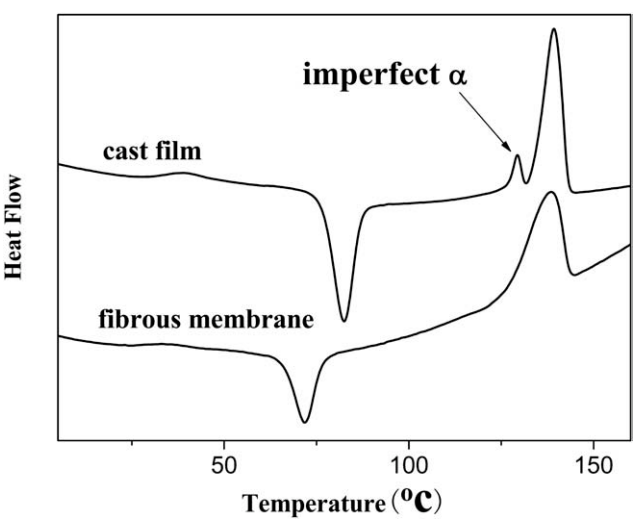

Figure 5 DSC curves of PLLA/PCL (1/1) blend cast film and electrospun fibrous membrane.

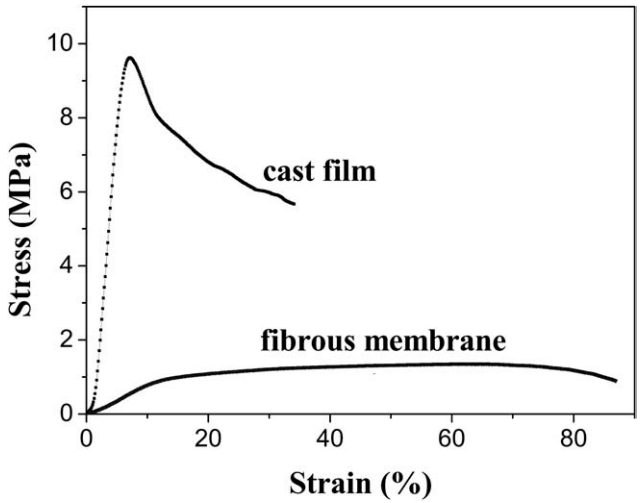

Figure 6 Tensile stress–strain curves of the electrospun fibrous membrane and cast films of PLLA/PCL (1/1) blend.

indicate that the rapid solidification of the polymer solution during electrospinning hinders crystallization. These results are consistent with the above XRD analysis.

Porosity and mechanical properties

Porosity and mechanical properties are important for tissue scaffolds. The porosity of the electrospun PLLA/PCL (1/1) blend fibrous membrane is high at 82%. Figure 6 shows the tensile stress–strain curves of the electrospun fibrous membrane and cast film, and their Young's modulus, tensile strength, and elongation-at-break are listed in Table II. Because the electrospun PLLA/PCL (1/1) blend fibrous membrane has higher porosity and lower crystallinity, its Young's modulus and tensile strength are reduced to 6.46 MPa and 1.21 MPa from 89.0 MPa and 9.4 MPa of the PLLA/PCL (1/1) blend cast film, but its elongation-at-break increases to 85.6% from 32.4% of the cast film. The high porosity and large ductility characteristics of the electrospun PLLA/PCL (1/1) blend fibrous membrane have made it a strong candidate for use as tissue scaffolds.

TABLE II
Mechanical Properties of Electrospun Fibrous Membrane and Cast Film of PLLA/PCL (1/1) Blend

Mechanical properties	Young's modulus (MPa)	Tensile strength[a] (MPa)	Elongation-at-break (%)
Cast film	89.0 ± 4.5	9.4 ± 4.3	32.4 ± 3.5
Electrospun fibrous membrane	6.46 ± 0.9	1.21 ± 0.1	85.6 ± 8.6

[a] Based on the maximum stress of the respective stress–strain curve.

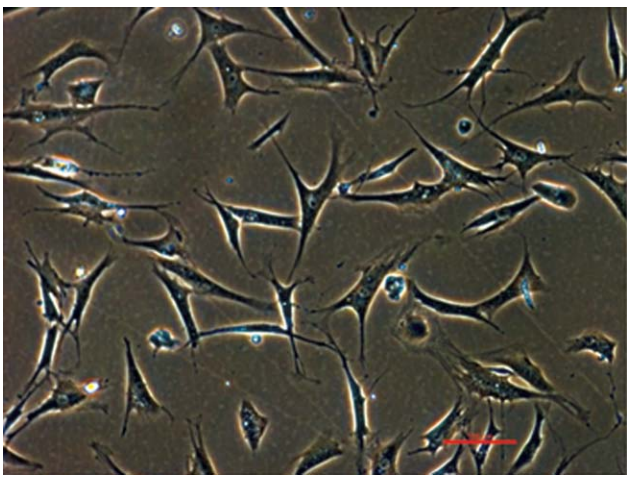

Figure 7 Optical morphology of ADSCs in conventional culture (magnification: ×200). [Color figure can be viewed in the online issue, which is available at wileyonlinelibrary.com.]

Cell morphology

The above results indicate that the electrospun PLLA/PCL blend fibers prepared by PLLA/PCL (1/1) blend with a solution concentration of 10 wt %, applied voltage of 20 kV, and TCD of 15 cm exhibit a defect-free morphology and uniform diameter of 780 ± 24 nm. Consequently, these optimal fibers were chosen for *in vitro* biocompatibility experiments as follows.

In this study, the morphology and interactions between ADSCs and PLLA/PCL blend fibrous scaffolds were examined by using inverted phase contrast microscopy and SEM. Figures 7 and 8 show typical morphologies of ADSCs in conventional culture and their attachment and growth on the PLLA/PCL fibrous scaffolds. It can be clearly seen in Figure 7 that ADSCs are triangular and polygonal, approximately 100∼150 μm in size, and uniformly dispersed in a monolayer with refraction lights around and beside the lipid droplets.[32] After being seeded on the PLLA/PCL fibrous scaffolds for 1 day, most ADSCs do not adhere to the fibers yet, but they grow to typical elongated morphology [Fig. 8(a,b)]. At 3 days, the ADSCs expanded on the fibrous scaffolds with a pattern of pseudopods as shown in Figure 8(c,d). After 7 days, an increasing number of cells grow along the fiber orientation direction, forming a three-dimensional network with a fibrous pattern [Fig. 8(e,f)]. In addition, the fibers swell slightly during cell culturing, and the fiber morphology changes owing to the absorption of the culture medium and possibly cell traction. However, more importantly, the PLLA/PCL blend fibers are biocompatible with ADSCs and are a good candidate scaffold for tissue engineering.

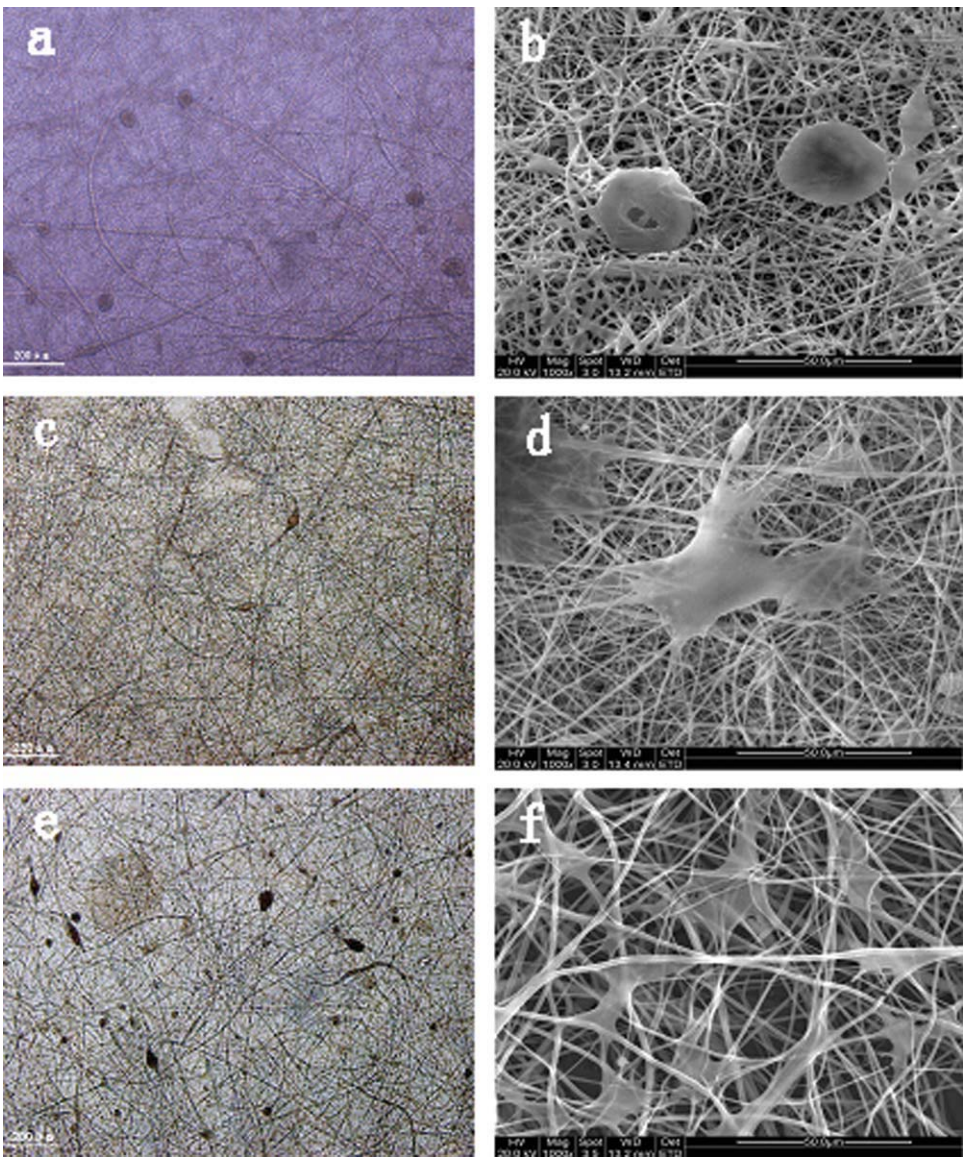

Figure 8 Morphology ADSCs on scaffolds after seeding for 1 day [(a) by inverted phase contrast microscopy (IPCM) and (b) by SEM], 3 days [(c) by IPCM and (d) by SEM], and 7 days [(e) by IPCM and (f) by SEM] (magnification: IPCM ×100; and SEM ×1000). [Color figure can be viewed in the online issue, which is available at wileyonlinelibrary.com.]

Cell proliferation, viability, and attachment

MTT assay is commonly used in cell proliferation *in vitro* and drug susceptibility testing of living cells by measuring the OD, which indirectly reflects the number of living cells. As shown in Figure 9, the curves of proliferation of both seeding and nonseeding ADSCs are very close to each other in the time range from 1 to 7 days, and that all OD values are higher than 0.05. The results indicate that the electrospun PLLA/PCL blend fibrous scaffolds have no toxic effect on proliferation of ADSCs.

Compared with MTT assay, live/dead cell staining served as a more intuitive assay. Figure 10 shows stained ADSCs seeding on PLLA/PCL blend fibrous scaffold for 1 day and 7 days. Obviously, live ADSCs cultured on scaffold are safely viable, and the dead cells are very few on the scaffold. During this time, ADSCs colonize the scaffolds and form a homogenous monolayer. Quantitatively, the percentage values (P_{Live}) of live ADSCs without and with scaffold at 1 day are 91.5% ± 9.2% and 89.7% ± 7.5%, respectively [Fig. 11(a)]. At 7 days, the P_{Live} values of live ADSCs without and with the scaffold, respectively, increase to 96.3% ± 3.0% and 94.4% ± 2.5%. The results demonstrate that the electrospun PLLA/PCL blend fibrous scaffolds provide ADSCs with a supportive interface to survive, and their fibrous structure is favorable for the ADSCs viability similar to native tissues.

Also from Figure 11(a), the attachment density (C_{Attach}) of ADSCs on the electrospun PLLA/PCL

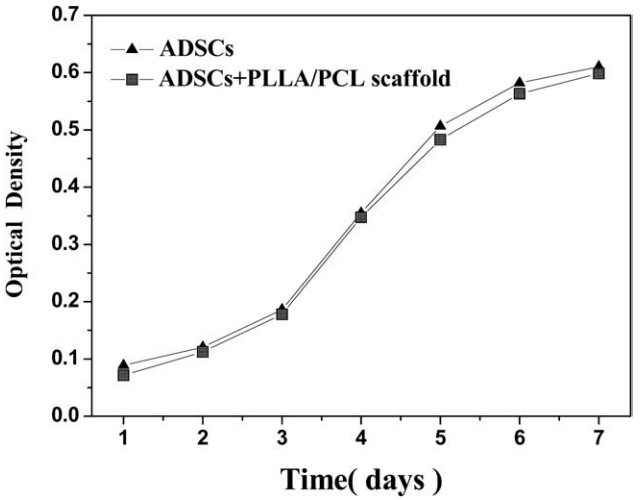

Figure 9 Proliferation curves of ADSCs by MTT assay.

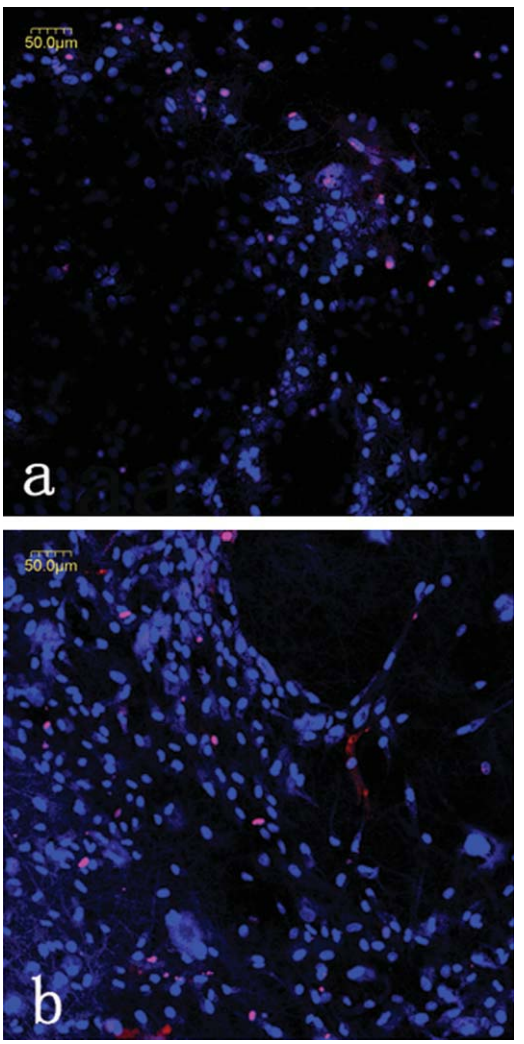

Figure 10 Live/dead cells staining of ADSCs on PLA/PCL blend fibrous scaffold after seeding for (a) 1 day and (b) 7 days. The live ADSCs stained blue and dead cells red (magnification: ×100). [Color figure can be viewed in the online issue, which is available at wileyonlinelibrary.com.]

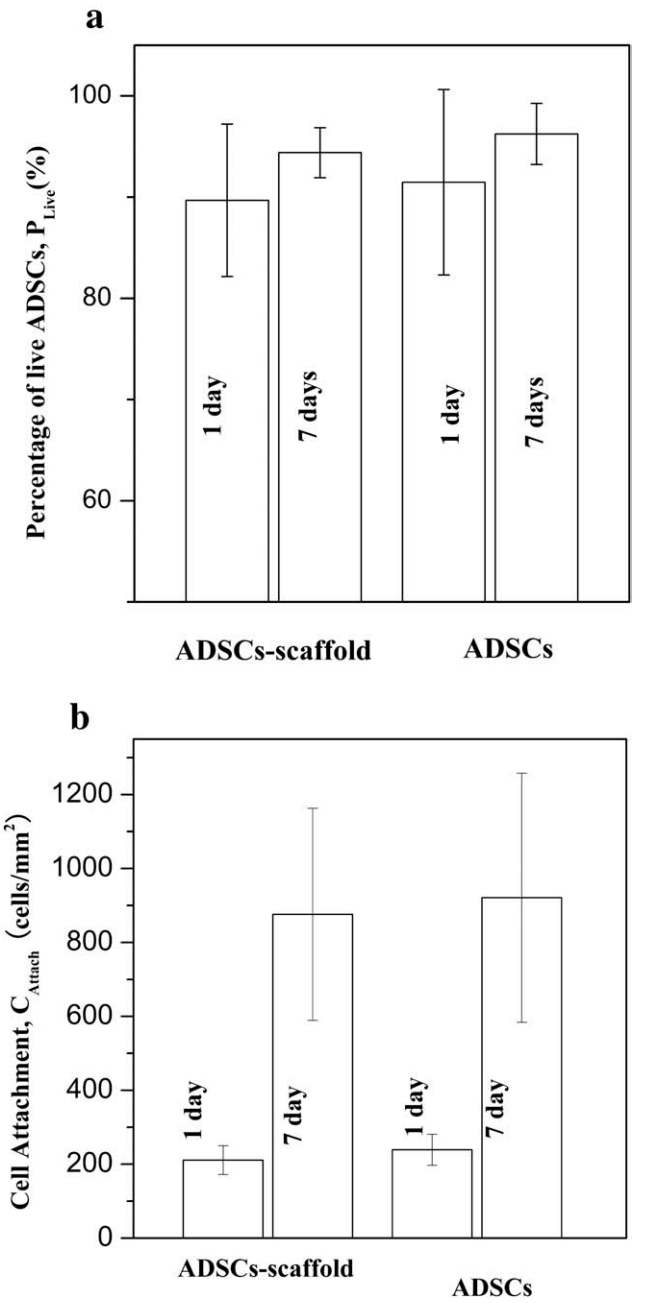

Figure 11 (a) Percentages of live ADSCs at 1 day and 7 days. (b) ADSCs attachment density at 1 day and 7 days.

blend fibrous scaffolds is 211 ± 39 cells/mm^2 at 1 day, which is close to 239 ± 42 cells/mm^2 of ADSCs without scaffolds. Similar to the survivability of ADSCs, the C_{Attach} values of live ADSCs without and with the scaffold at 7 days increase to 921 ± 337 and 876 ± 287 cells/mm^2, respectively. It should be noted that C_{Attach} of live ADSCs on scaffold at 7 days represents a lower estimated value because the live cells are too crowded to be accurately counted. Based on the C_{Attach} values of live ADSCs without and with the scaffold, it is concluded that PLLA/PCL blend fibrous scaffolds provide a favorable

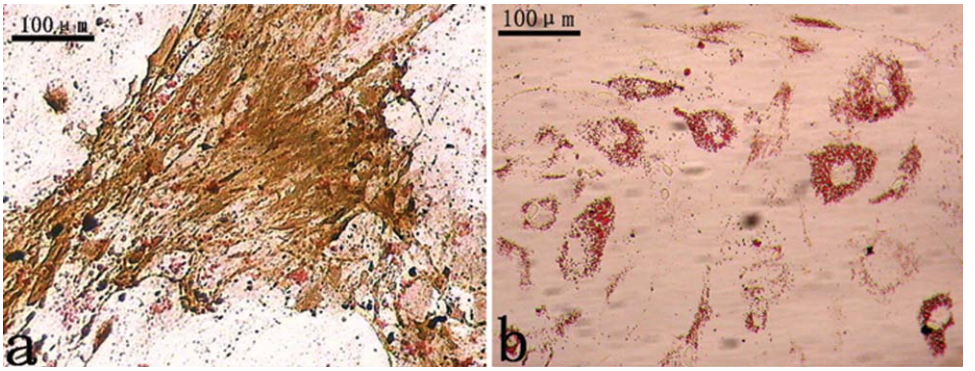

Figure 12 Immunohistochemistry staining for characterization of osteogenesis and adipogenesis: (a) Von Kossa staining for osteogenic differentiation. The mineralized ECM stained brown; (b) Oil red O staining for adipogenic differentiation. The accumulated lipid stained red (magnification: ×200). [Color figure can be viewed in the online issue, which is available at wileyonlinelibrary.com.]

environment similar to conventional culture. Generally, a suitable scaffold for tissue engineering must be biocompatible to allow cell attachment, proliferation, and ultimate viability. The above results indicate that the electrospun PLLA/PCL blend fibrous scaffolds can stabilize the proliferation and attachment of ADSCs.

Differentiation of ADSCs on scaffolds

The pluripotency of ADSCs on scaffolds was assessed by immunohistochemistry. The positive expression in Figure 12 confirms the multilineage differentiation of ADSCs on scaffolds. In Figure 12(a), von Kossa staining shows calcium deposition in the ECM, which indicates osteogenesis. In Figure 12(b), oil red O staining shows the lipid accumulation in the ECM, which indicates adipogenesis. In the tissue engineering field, a biocompatible scaffold should meet the requirement to support the stem cell to differentiate into desired cell lineage. Similar with the pluripotency of ADSCs in conventional culture and expansion,[30-32,34] the multilineage differentiation of ADSCs on such scaffold indicates the prospect to replace the native ECM for tissue engineering.

CONCLUSIONS

The electrospun PLLA/PCL blend fibers with defect-free morphology and uniform diameter can be prepared by PLLA/PCL (1/1) blend with a solution concentration of 10 wt %, applied voltage of 20 kV, and TCD of 15 cm. Owing to the rapid solidification of polymer solution during electrospinning, the crystallinity of electrospun PLLA/PCL blend fibers is much lower than that of the PLLA/PCL blend cast films. The optimal electrospun PLLA/PCL blend fibrous membranes can be used as a good scaffold for ADSCs proliferation, viability, attachment, and differentiation because of their good biocompatibility and nontoxic effects. Further work is under way to extend our studies to *in vivo* evaluation of the electrospun PLLA/PCL fibers to understand the interactions between cells and biomaterials at the molecular level.

The authors thank HUST Analysis and Testing Center for access to its SEM and XRD facilities.

References

1. Huang, Z. M.; Zhang, Y. Z.; Kotaki, M.; Ramakrishna, S. Compos Sci Technol 2003, 63, 2223.
2. Sill, T. J.; von Recum, H. A. Biomaterials 2008, 29, 1989.
3. Doshi, J.; Reneker, D. H. J Electrostat 1995, 35, 151.
4. Reneker, D. H.; Chun, I. Nanotechnology 1996, 7, 216.
5. Lu, X. F.; Wang, C.; Wei Y. Small 2009, 5, 2349.
6. Jin, Y.; Yang, D. Y.; Kang, D. Y.; Jiang, X. Y. Langmuir 2010, 26, 1186.
7. Desai, K.; Kit, K.; Li, J. J.; Zivanovic, S. Biomacromolecules 2008, 9, 1000.
8. Fong, H.; Chun, I.; Reneker, D. H. Polymer 1999, 40, 4585.
9. Aluigi, A.; Vineis, C.; Varesano, A.; Mazzuchetti, G.; Ferrero, F.; Tonin, C. Eur Polym J 2008, 44, 2465.
10. Pamula, E.; Menaszek, E. J Mater Sci Mater Med 2008, 19, 2063.
11. Cohn, D.; Salomon, A. H. Biomaterials 2005, 26, 2297.
12. Huang, M. H.; Li, S. M.; Vert, M. Polymer 2004, 45, 8675.
13. Garkhal, K.; Verma, S.; Jonnalagadda, S.; Kumar, N. J Polym Sci Part A: Polym Chem 2007, 45, 2755.
14. Yang, F.; Murugan, R.; Wang, S.; Ramakrishna, S. Biomaterials 2005, 26, 2603.
15. Lee, K. H.; Kim, H. Y.; Khil, M. S.; Ra, Y. M.; Lee, D. R. Polymer 2003, 44, 1287.
16. Na, Y. H.; He, Y.; Shuai, X.; Kikkawa, Y.; Doi, Y.; Inoue, Y. Biomacromolecules 2002, 3, 1179.
17. López-Rodríguez, N.; López-Arraiza, A.; Meaurio, E.; Sarasua, J. R. Polym Eng Sci 2006, 46, 1299.
18. Aslan, S.; Calandrelli, L.; Laurienzo, P.; Malinconico, M.; Migliaresi, C. J Mater Sci 2000, 35, 1615.
19. Mo, X. M.; Xu, C. Y.; Kotaki, M.; Ramakrishna, S. Biomaterials 2004, 25, 1883.
20. Xu, C. Y.; Inai, R.; Kotaki, M.; Ramakrishna, S. Biomaterials 2004, 25, 877.
21. Xu, C. Y.; Inai, R.; Kotaki, M.; Ramakrishna, S. Tissue Eng 2004, 10, 1160.

22. Kwon, I. K.; Kidoaki, S.; Matsuda, T. Biomaterials 2005, 26, 3929.
23. Vaz, C. M.; van Tuijl, S.; Bouten, C. V. C.; Baaijens, F. P. T. Acta Biomater 2005, 1, 575.
24. Ajami-Henriquez, D.; Rodríguez, M.; Sabino, M.; Castillo, R. V.; Müller, A. J.; Boschetti-de-Fierro, A.; Abetz, C.; Abetz, V.; Dubois, P. J Biomed Mater Res A 2008, 87, 405.
25. Calandrelli, L.; Calarco, A.; Laurienzo, P.; Malinconico, M.; Petillo, O.; Peluso, G. Biomacromolecules 2008, 9, 1527.
26. Rohman, G.; Pettit, J. J.; Isaure, F.; Cameron, N. R.; Southgate, J. Biomaterials 2007, 28, 2264.
27. Baker, S. C.; Rohman, G.; Southgate, J.; Cameron, N. R. Biomaterials 2009, 30, 1321.
28. Musyanovych, A.; Schmitz-Wienke, J.; Mailänder, V.; Walther, P. Landfester K. Macromol Biosci 2008, 8, 127.
29. Li, W. J.; Tuli, R.; Okafor, C.; Derfoul, A.; Danielson, K. G.; Hall, D. J.; Tuan, R. S. Biomaterials 2005, 26, 599.
30. Gimble, J. M.; Katz, A. J.; Bunnell, B. A. Circ Res 2007, 100, 1249.
31. Zuk, P. A.; Zhu, M.; Ashjian, P.; De Ugarte, D. A.; Huang, J. I.; Mizuno, H.; Alfonso, Z. C.; Fraser, J. K.; Benhaim, P.; Hedrick, M. H. Mol Biol Cell 2002, 13, 4279.
32. Zuk, P. A.; Zhu, M.; Mizuno, H.; Huang, J.; Futrell, J. W.; Katz, A. J.; Benhaim, P.; Lorenz, H. P.; Hedrick, M. H. Tissue Eng 2001, 7, 211.
33. Wang, Y.; Bian, Y. Z.; Wu, Q.; Chen, G. Q. Biomaterials 2008, 29, 2858.
34. Gimble, J.; Guilak, F. Cytotherapy 2003, 5, 362.
35. Chen, H.; Snyder, J. D.; Elabd, Y. A. Macromolecules 2008, 41, 128.
36. Rezgui, F.; Swistek, M.; Hiver, J. M.; G'Sell, C.; Sadoun, T. Polymer 2005, 46, 7370.
37. Zhou, H. J.; Green, T. B.; Joo, Y. L. Polymer 2006, 47, 7497.
38. Sarasua, J. R.; López-Arraiza, A.; Balerdi, P.; Maiza, I. Polym Eng Sci 2005, 45, 745.